Journal of Solid State Chemistry 184 (2011) 805–810

Contents lists available at ScienceDirect

Journal of Solid State Chemistry

journal homepage: www.elsevier.com/locate/jssc

Electrostatic interaction effect for human DNA separation with functionalized mesoporous silicas

Hong Kyung Choi [a,b], Jeong Ho Chang [a,*], Il Hwan Ko [a], Jin Hyung Lee [a], Bong Yong Jeong [a], Jong Hee Kim [a], Jung Bae Kim [b]

[a] Korea Institute of Ceramic Engineering and Technology, Seoul 153-801, Republic of Korea
[b] Department of Chemical and Biological Engineering, Korea University, Seoul 136-701, Republic of Korea

ARTICLE INFO

Article history:
Received 13 October 2010
Received in revised form
30 January 2011
Accepted 6 February 2011
Available online 12 February 2011

Keywords:
Functionalized mesoporous silicas
DNA separation
Electrostatic interaction
Solid-state NMR
Confocal microscope

ABSTRACT

This work describes the development of highly efficient human DNA separation with functionalized mesoporous silica (FMS) materials. To demonstrate the electrostatic interaction effect between the target DNA molecules and FMS, three aminofunctionality types comprised of a mono-, a di-, and a tri-amine functional group were introduced on the inner surfaces of mesoporous silica particles. Systematic characterization of the synthesized materials was achieved by solid-state ^{29}Si and ^{13}C-NMR techniques, BET, FT-IR, and XPS. The DNA separation efficiency was explored via the function of the amino-group number, the amount used, and the added NaCl concentration. The DNA adsorption yields were high in terms of the use of triaminofunctionalized FMS at the 10 ng/L level, and the DNA desorption efficiency showed the optimum level at over 3.0 M NaCl concentration. The use of FMS in a DNA separation process provides numerous advantages over the conventional silica-based process.

1. Introduction

The application of silica and silica-based materials to life-science technologies is attracting attention from numerous research fields, including biotechnology, and nanomaterial science. These materials have been assessed as drug or gene delivery systems, bio-separation agents, diagnostic agents, and as sensors due to their high surface areas and straightforward surface modification [1–8]. One of the recent interests in bio-applications focused on the separation and purification of specific bio-pharmaceuticals such as DNA and protein from multi-component mixtures [9,10]. DNA separation is especially important for the sequencing of genomes, DNA fingerprinting, the identification of pathogens, and numerous types of genetic assays that are used to identify diseases. Current DNA separation methods engender several drawbacks that make them unsuitable for the manufacturing of pharmaceutical-grade materials. They often involve the use of some or all of the following: solvents; toxic chemicals such as cesium chloride, ethidium bromide, phenol, and chloroform; or animal-derived enzymes such as ribonuclease A and lysozyme that are either not approved or not recommended by regulatory agencies. Moreover, the research of the utilization of MNPs has been interesting and burgeoning in the fields of the bio-separation due to the convenient and time-saving process. Especially, iron-oxide-based magnetic nanomaterials have been used for the magnetic separation in DNA and proteome researches because of the good hydrophilicity, biocompatibility, and nontoxicity. However, the MNPs-based process suffers from the low separation efficiency due to the agglomeration and low surface reactivity. A common limitation of the commercial matrix is also the low capacity of DNA due to the inability of large molecules to penetrate porous beads, there have been no reports of a matrix being used to separate DNA simultaneously. Consequently, there is a need for large-scale processes to manufacture highly pure DNA, and the requirements of regulatory agencies regarding purity, potency, safety, and efficacy must be achieved.

Hence, we tried to demonstrate novel approach with ordered mesoporous silica (MS) materials, in which they have the high surface areas by the homogeneous nanopores and channels. The lots of nanopores and high surface areas are suitable for enhancement of separation efficiency. Actually, the comparison of surface areas between MS and MNPs shows much difference; the MS has 800–1300 m^2/g, but the MNPs has 10–30 m^2/g. Furthermore, lots of silanol group ($-OH$) at the surface of MS are suitable for observation of electrostatic interaction between solid materials and target biomolecules by surface modification.

In this work, we prepared poly-amino group assembled FMS as a function of the number of amino groups tailored for mono-, di-, and tri-aminofunctionality to demonstrate the highly efficient DNA separation efficiency. The application of FMS to DNA separation research provides many immediate advantages, including higher surface-to-volume areas, enhanced binding efficiency, and

* Corresponding author.
E-mail address: jhchang@kicet.re.kr (J.H. Chang).

0022-4596/$ - see front matter Crown Copyright © 2011 Published by Elsevier Inc. All rights reserved.
doi:10.1016/j.jssc.2011.02.005

higher specificity. We expect that the aminofunctionalized FMS should be very useful in DNA separation processes compared to conventional silica-based process due to its simple operation and high-throughput process.

2. Experimental

2.1. Materials

Pluronic P123 (PEO_{20}-PPO_{70}-PEO_{20}) was purchased from BASF (Korea Branch). Tetraethyl orthosilicate (99%), aminopropyl trimethoxysilane (99%), and toluene (99%) were purchased from Aldrich. *N*-[3-(trimethoxysilyl)propyl]-ethylenediamine (99%) and *N*-[3-(trimethoxysilyl)propyl]-diethylenetri-amine (99%) were purchased from Gelest. All other chemicals were of extra pure analytical grade and were used without further purification. The phosphate buffers (PB) used here were a mixture of 2.17 mM KH_2PO_4 and 7.61 mM Na_2HPO_4. All aqueous solutions were prepared with double-distilled water, obtained from a Milli-Q water purifying system (18.3 MΩ cm).

2.2. Instrumental analyses

The nitrogen adsorption and desorption isotherms were measured using a Quantachrome Autosorb-6 system. The sample was pretreated in a vacuum line. The pore size distributions were calculated from an analysis of the adsorption branch of the isotherm using the Barrett–Joyner–Halenda (BJH) method. The XPS measurement was obtained using a SSI 2803-S spectrometer with Al *K*α. The X-rays proceeded at 12 kV and 20 mA. All core-level spectra were obtained at a photoelectron take-off angle of 35° with respect to the sample surface. To compensate the surface charging effect, all binding energies were referenced to a C 1*s* neutral carbon peak at 284.6 eV. The N 1*s* peaks were deconvoluted into components consisting of a Gaussian line shape Lorentzian function. Confocal laser scanning microscopy was performed using a LEICA-TCS SP2 AOBS model. Cy-5 labeled DNA-bound aminofunctionalized FMS were excited at 650 nm and their emission spectra were captured.

2.3. Synthesis of aminofunctionalized FMS

In a typical preparation, 4.0 g of Pluronic P123 was dissolved in 30 g of water and 120 g of 2 M HCl, and 8.5 g of tetraethyl orthosilicate (TEOS) was then added to the solution at 40 °C. The mixture was aged in a stainless-steel bomb at 120 °C overnight without stirring. The solid product was filtered, washed with excess water, and air-dried at room temperature. Calcination was carried out in air at 550 °C for 6 h. To represent the functional monolayers of aminosilanes, 5.0 g of mesoporous silicas in 150 mL of toluene that contained 1.60 mL of deionized water and 1.475 mmol of the aminosilanes-aminopropyl trimethoxysilane(APTMS), *N*-[3-(trimethoxysilyl)propyl]-ethylenediamine(TMPEA), and *N*-[3-(trimethoxysilyl)propyl]-diethylenetri-amine (TMPDT) were added and refluxed for 6 h. The resulting white powder was filtered, washed with toluene, and air-dried. The hybrid material was filtered, washed with toluene and then dried under a vacuum at 70 °C before use. The white powder was finally filtered, washed with toluene, and dried in the air and in a vacuum.

2.4. DNA adsorption and desorption experiments

For DNA adsorption and desorption work with FMS, blood is chemically lysed to be released from the cells. Here, proteinase K (10 μL of a 10 mL aqueous solution) was added to whole blood and the solution was diluted to 300 μL in a cell lysis buffer. After centrifugation for 10 min, the supernatant blood waste was removed and washed. The supernatant was again transferred to a new tube, and 600 μL of a binding buffer was added. The solution was stirred for 10 min and centrifuged for 2 min at 12,000 rpm. Finally TE buffer (10 mM Tris–HCl, 1 mM EDTA, pH 8) was added and then centrifuged for 1 min. DNA adsorption and desorption experiments were conducted in which a total of 50 μL crude cell lysates, 10 μL aminofunctionalized FMS (10 mg/mL), and 50 μL TAE buffer (40 mM Tris, 20 mM acetic acid, 1 mM EDTA, pH 8.0) were mixed and incubated for 10 min at the laboratory temperature. The aminofunctionalized FMS with adsorbed DNA was then separated, the supernatant was collected, and the aminofunctionalized FMS were washed with 500 μL of TAE buffer and quickly dried. DNA captured by the aminofunctionalized FMS

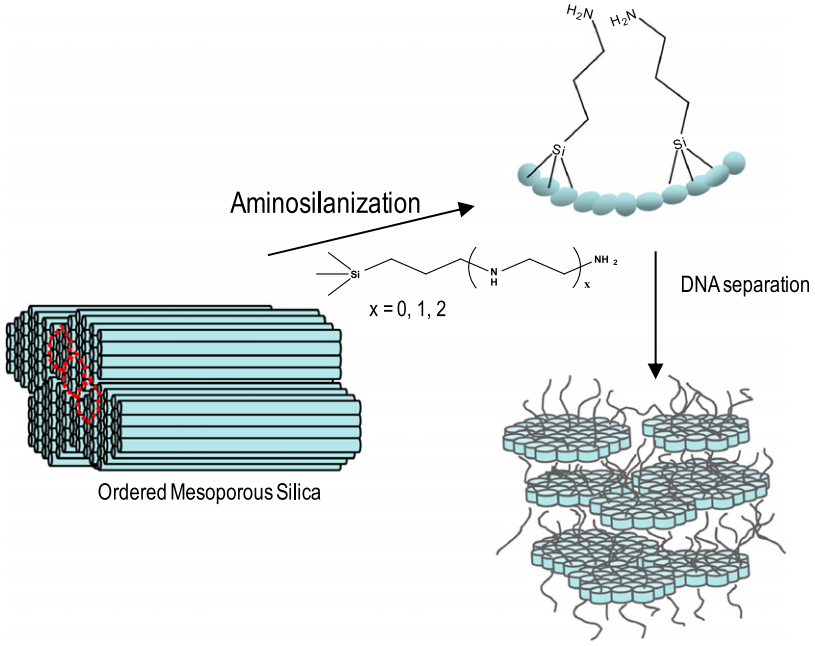

Scheme 1. Schematic representation of high efficient DNA separator with functionalized ordered mesoporous silica materials through the aminosilanization.

was eluted into 50 μL of TAE buffer. DNA in the eluate (1 μL) was used as a DNA matrix for PCR amplification and for agarose gel electrophoresis. The nucleic acid concentration in the solution could be readily calculated from absorbance at 260 nm. Agarose gel electrophoresis was achieved from a horizontal gel electrophoresis unit in TAE buffer including 1% agarose gel and 0.1 μg/mL ethidium bromide (EtBr). Electrophoresis was carried out for each sample at 100 V for 20 min including the supernatants before/after adsorption, washing, and the desorption work.

3. Results and discussion

The route for DNA separation with aminofunctionalized FMS is shown in Scheme 1. The starting mesoporous silicas were prepared according to the method reported in the literatures [11,12]. The synthesized mesoporous silica have surface areas of up to 862 m^2/g and pore sizes of 95 and 66 Å on the adsorption and desorption branches, respectively. The self-assembly of amine groups on mesoporous silica particles was introduced in previous reports by the authors [13–15]. Three types of aminosilanes, namely APTMS, TMPEA, and TMPDT were used for mono-amine (MA-FMS), di-amine (DA-FMS), and tri-amine (TA-FMS), respectively. DNA adsorption and desorption experiments were conducted in TAE buffer (40 mM Tris, 20 mM acetic acid, 1 mM EDTA, pH 8.0). DNA captured by the aminofunctionalized FMS was eluted into a TAE buffer. Subsequently, the concentration of DNA in the solution could be readily calculated from absorbance at 260 nm.

A transmission electron microscopy (TEM) image of a 9.5 nm mesoporous silica substrate showed the uniform sizes of the pores and channels, which exhibited a hexagonal array of lattice fringes as well as parallel fringes corresponding to the side-on view of the pores (Fig. 1(a)). As the aminosilanes were deposited on the mesoporous silica substrate, the surface areas and pore sizes were reduced. Fig. 1(b) shows plots of the relationship among the pore size, zeta potential, and BET surface areas as a function of the amino group. As the aminofunctionality increased, the pore sizes decreased linearly and were regularly distributed from 9.5 to 4.8 nm. According to the BET measurement results, the surface areas of the aminofunctionalized FMS showed a drastic decrease from 782 to 49 m^2/g due to the increase in the surface coverage caused by the tri-aminofunctionality. Zeta potential measurements showed an increase in the zeta potential values as a function of the amino group, from −25 to 38 mV. Nitrogen adsorption and desorption BET isotherms as a function of the amino group showed a microporous pattern from a mesoporous pattern of a type IV isotherm with H2-type loops (Fig. 1(c)).

X-ray photoelectron spectroscopy (XPS) capable of showing the wide scan spectra of aminofunctionalized FMS was demonstrated for the characterization of the molecularly assembled surfaces (Fig. 2(a)). The spectrum showed that Si electronic configuration peaks appear at 149 and 100 eV for 2*s* and 2*p*, respectively. After aminofunctionalization of the surface of mesoporous silica particles, two peaks of N 1*s* and C 1*s* were initially observed at 399 and 285 eV, respectively. For a quantitative analysis of the new C and N peaks, the atomic concentration profiles in XPS were calculated. The result showed that the concentration of N 1*s* of aminofunctionalized FMS increased to 4.5%, 8.0%, and 9.9% for MA-FMS, DA-FMS, and TA-FMS, respectively. Moreover, the atomic concentration of C 1*s* increased to 35.7%, 36.0%, and 36.5% for MA-FMS, DA-FMS, and TA-FMS, respectively. These results are in good agreement with those of FT-IR measurements. The FT-IR spectra of aminofunctionalized FMS were obtained by the attenuated total reflectance (ATR) method (Fig. 2(b)). The OH stretching vibrations

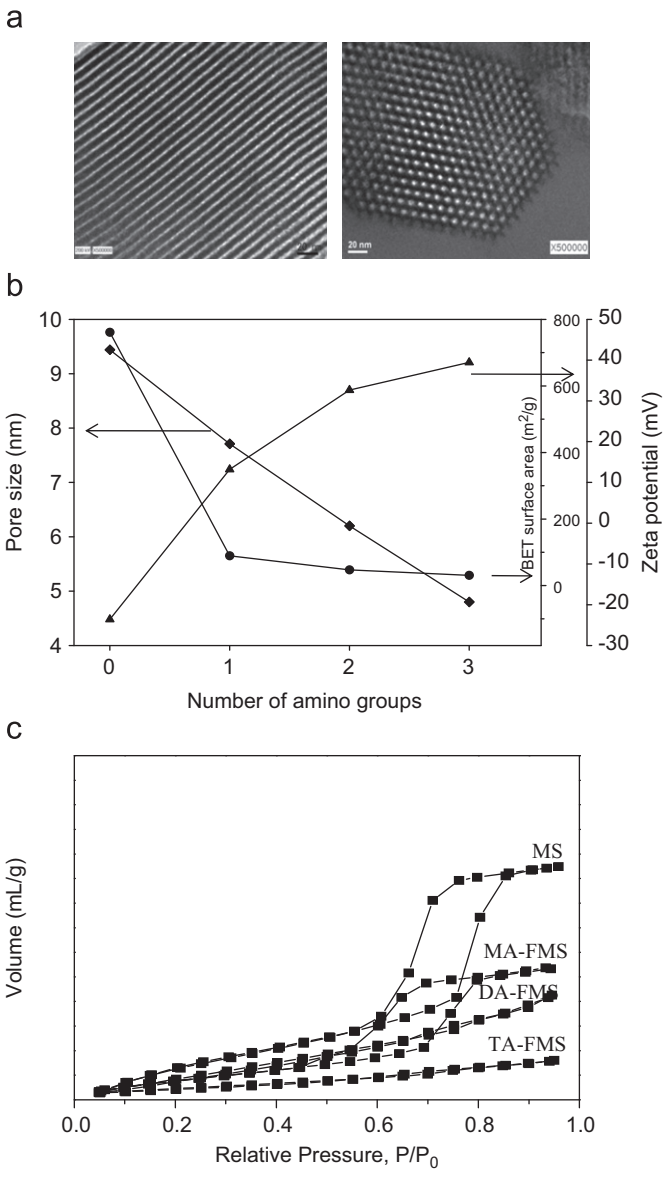

Fig. 1. (a) TEM images of mesoporous silicas, (b) relationship among the BET pore sizes, surface areas, and zeta-potentials, and (c) BET isotherms as a function of the number of aminofunctionaization.

of the Si-OH group appeared at 830–1110 cm^{-1} and vibrations for the Si-OH and Si-H appeared at 800–950 cm^{-1}. The primary functional group of the FMS, the amino group, shows that the specific functional stretching frequencies are widely observed at their wavenumbers. For example, the N–H and C–N stretching of the primary amide was approximately 3600–3900 and 1500–1600 cm^{-1}, respectively. The main characteristic peak of the poly-amino-FMS as a function of amino-group number is C–N vibration modes, in which their intensity is proportional to the number of surface amine groups. Consequently, the C–N intensity of TA-FMS is stronger than those of the other samples such as DA-FMS and MA-FMS.

To confirm the formation of aminosilane monolayers on the surface of mesoporous silicas, both solid-state ^{29}Si and ^{13}C-NMR techniques were utilized to provide chemical information in relation to the localized silicon and carbon environments (Fig. 3). Single-pulse ^{29}Si-NMR spectra were obtained via long recycle times (30 s) of the Bloch decay-pulse (single-pulse

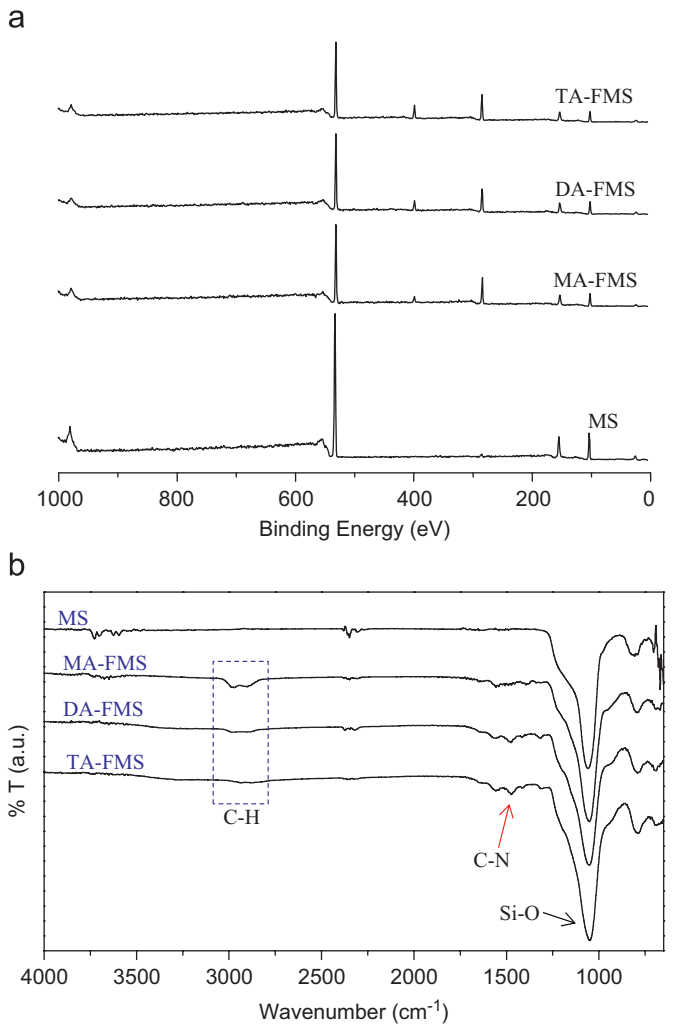

Fig. 2. (a) XPS spectrum and (b) FT-IR spectrum by ATR method as a function of the number of aminofunctionaization.

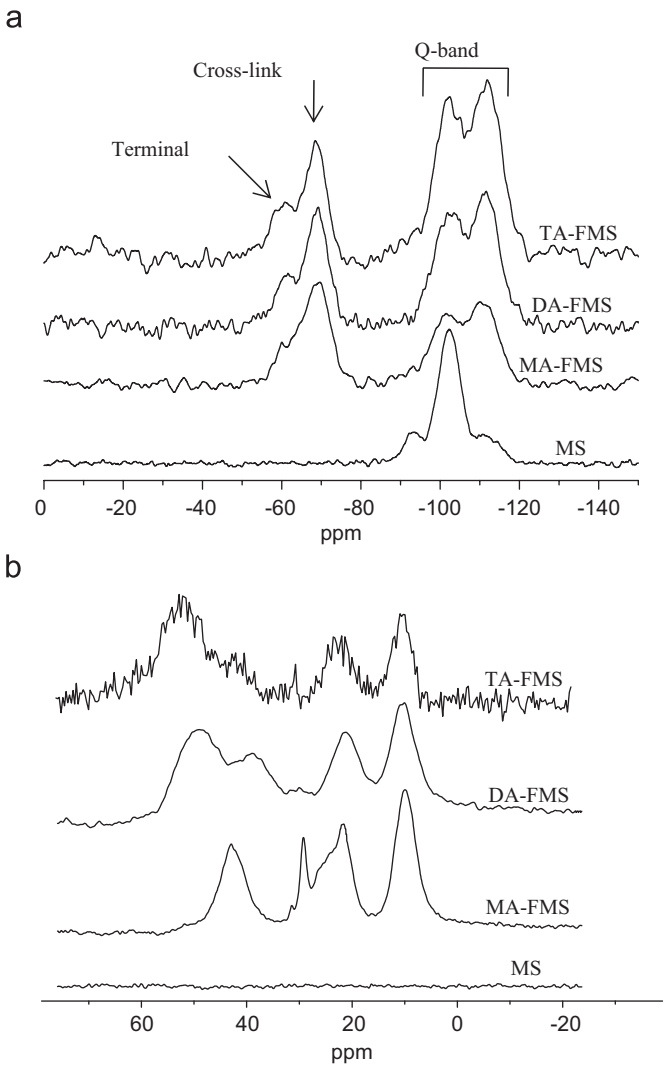

Fig. 3. The solid-state nuclear magnetic resonance spectrum: (a) ^{29}Si-NMR and (b) ^{13}C-NMR spectra as a function of the number of aminofunctionaization.

excitation). The initial ^{29}Si-NMR spectra of the mesoporous silicas were at −91, −102, and −112 ppm, corresponding to the $(HO)_2Si(OSi)_2$ (Q^2), $HOSi(OSi)_3$ (Q^3), and $Si(OSi)_4$ (Q^4) silicate species, in which Q^n represents silicon atoms bonded to n neighboring silicon atoms via Si–O–Si bonds. The high Q^3 peak is typical of mesoporous materials with high surface areas. After the formation of aminosilane monolayers on the mesoporous silicas, the Q^4 peak was significantly increased by the formation of $-(OSi)_4$ segments from aminosilanes. The ratios of the relative peak areas of the Q^4 and Q^3 signals for MA-FMS, DA-FMS, and TA-FMS are 1.2, 1.1, and 1.1, respectively. These ratios reveal that the aminosilanes monolayers on the mesoporous silicas were obtained in a process nearly identical to that of the hydrolysis and condensation reaction from each aminosilane used. Moreover, the siloxane peaks from three aminosilanes were newly observed in a range of −55 to −80 ppm, in which the resonance intensity of cross-linked siloxane near −70 ppm was shown to be stronger than that of terminal siloxane near −60 ppm, indicating a strong intermolecular chain-to-chain interaction (cross-link) between the aminosilanes and the mesoporous silica substrates. The cross-linking ratios, Si(cross-link)/Si(terminal), were 2.31, 2.27, and 1.94 for MA-FMS, DA-FMS, and TA-FMS, respectively. The single-pulse ^{13}C-NMR spectra along with the peak assignment were determined, and several features are noteworthy. When aminosilanes were formed the monolayers on the mesoporous silica, the chemical shifts of the major carbon backbones as bonded to silicon groups ($R–Si–C^1H_2C^2H_2C^3H_2$) were observed at 9.9, 21.9, and 42.8 ppm corresponding to C^1, C^2, and C^3, respectively. With the increase in the amino-group number, the chemical shifts of carbon atoms bonded to amino groups ($R–NH–CH_2$) shifted to higher fields while broadening and finally splitting.

The surface-modified mesoporous silica particles after aminofunctionalization were explored through the adsorption and desorption of human DNA (45,000 bp) based on the results from electrophoresis and spectroscopic analyses of ultraviolet absorbance measurements (Fig. 4). The effective DNA adsorption work was achieved with aminofunctionalized FMS as a function of the amount, in which the adsorption yield was dependent on the amount of FMS used. Furthermore, a greater aminofunctionality of the mesoporous silica particles showed greater DNA adsorption in the order of tri-amino (TA) > di-amino (DA) > mono-amino (MA) functionality due to the increase in the level of electrostatic interaction between the positive amino groups and the negative phosphate backbone of the DNA within the 10 ng/L of particle amounts. A spectroscopic analysis to explore the DNA separation work was also conducted using ultraviolet absorbance measurements with a resident (supernatant) solution after the

DNA binding at wavelengths of 260 nm, in which strong adsorption at 260 nm derived from the base part of the DNA proved that DNA was actually bound to the aminofunctionalized mesoporous silica particles (data is not shown here). A DNA desorption experiment was also conducted as a function of the concentration of NaCl salts. The conventional DNA desorption process is also associated with temperature rises and NaCl salt additions. The process adapted in this work sought to change the ionic strength for the dissociation using various molar concentrations of NaCl salt from 0.1 to 3.0 M, in which the sodium salt interacted with the phosphate backbone of the DNA and decreased the bond strength of DNA-bound aminofunctionalized mesoporous silica particles. The solution of the lower NaCl molar concentration did not dissociate the bounded DNA much, but the MA-FMS sample showed good dissociation (it was easily broken down) due to the weak electrostatic interactions. Consequently, additional aminofunctionalized FMS was required to dissociate the DNA with the addition of sodium salt. The DNA dissociation property of the aminofunctionalized FMS showed the order of MA > DA > TA functionality. The effective DNA dissociation did not depend on the functionality over a concentration of 3.0 M NaCl. All adsorbed DNA on FMS was perfectly dissociated because the ionic strength between the FMS and target DNA was fully weakened to dissociate, thus allowing DNA desorption.

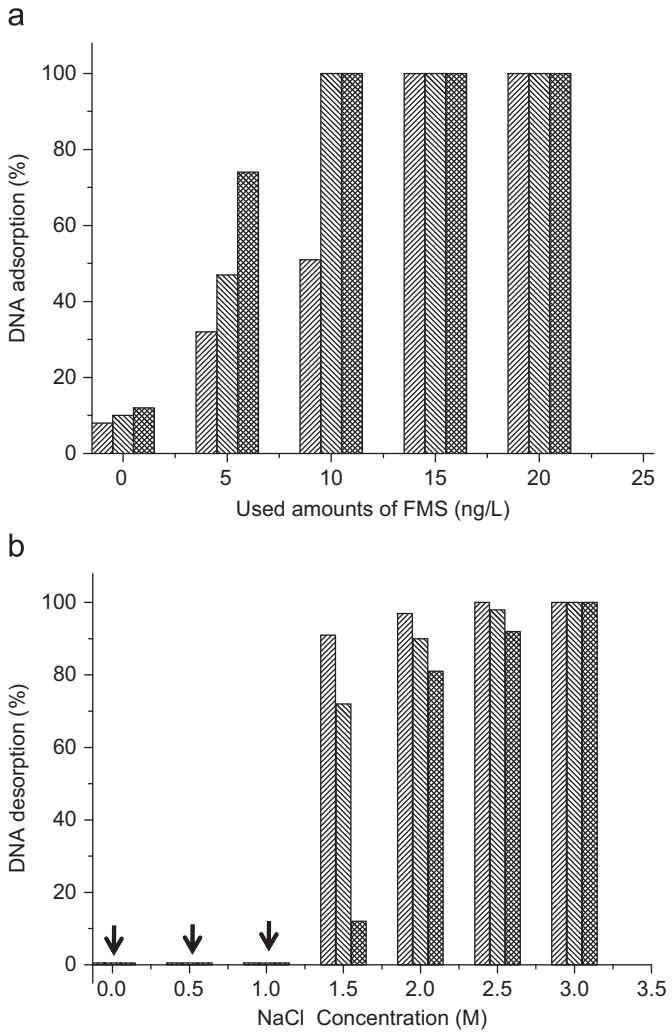

Fig. 4. (a) DNA adsorption yields as a function of used FMS particles, (b) DNA desorption yields as a function of NaCl concentration. (▨ : MA-Msp, ▨ : DA-Msp, and ■ : TA-Msp).

Further studies of the electrostatic interaction between the target DNA labeled by cyanine (Cy-5) and aminofunctionalized FMS were achieved via confocal microscopy (Fig. 5). The confocal laser scanning microscope images provided the DNA adsorption efficiency as a function of the level of aminofunctionality. With an increase in the level of aminofunctionality, the red color from the adsorbed Cy-5 labeled DNA covers the entire detection area due to the strong electrostatic binding with DNA. Moreover, the aminofunctionalized FMS appears to be aggregated to each other so as to adsorb the target DNA effectively.

4. Conclusion

A simple and convenient process was demonstrated for highly efficient and direct DNA separation with aminofunctionalized FMS. The introduction of hydrophilicity changes with aminosilanization on the surfaces of mesoporous silica particles, which enhances the DNA separation efficiency due to the amount of electrostatic interaction. The DNA separation efficiency was explored via the function of the amino-group number, particles size, amount of FMS used, and the NaCl concentration. The DNA adsorption yields were high in terms of the use of triaminofunctionalized FMS and the DNA desorption efficiency showed the optimum level at a NaCl concentration that exceeded 3.0 M. This preliminary study can enable the design and construction of an automatic system capable of high-throughput biomolecular purification with FMS particles. This can then be applied for clinical diagnoses and proteins/enzymes recognition processes using an appropriate surface modification technique.

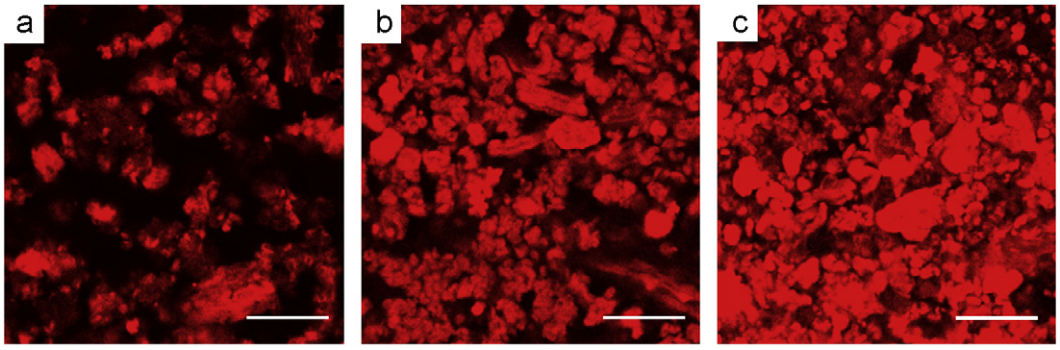

Fig. 5. Confocal laser scanning microscopy images of excited Cy-5-labeled DNA-bound aminofunctionalized FMS at 650 nm: (a) MA-FMS, (b) DA-FMS, (c) TA-FMS (the scale bar is 4 μm).

Acknowledgments

This work was supported by a grant from the Fundmental R&D Program for Core Technology of Materials funded by the Ministry of Knowledge Economy, Republic of Korea, and partially supported by Korea Institute of Ceramic Engineering and Technology (KICET).

References

[1] F. Torney, B.G. Trewyn, V.S.Y. Lin, K. Wang, Nat. Nantotechnol. 2 (2007) 295.
[2] I.I. Slowing, B.G. Trewyn, S. Giri, V.S.Y. Lin, Adv. Funct. Mater. 17 (2007) 1225.
[3] M. Han, X. Gao, J.Z. Su, S. Nie, Nat. Biotechnol. 19 (2001) 631.
[4] L. Josephson, J.M. Perez, R. Weissleder, Angew. Chem. Int. Ed. 40 (2001) 3204.
[5] L. Babes, B. Denizot, C. Tangguy, J. Jacques, L. Jeune, P. Jallet, J. Colloid Interface Sci. 212 (1999) 474.
[6] J. Allouche, M. Boissiere, C. Helary, J. Livage, T. Coradin, J. Mater. Chem. 16 (2006) 3120.
[7] X.D. Tong, B. Xue, Y. Sun, Biotechnol. Prog. 17 (2001) 134.
[8] M.D. Cuyper, M. Hodenius, Z.G.M. Lacava, R.B. Azevedo, M.D. Silva, P.C. Morais, M.H.A. Santana, J. Colloid Interface Sci. 245 (2002) 274.
[9] J.M. Perez, T. Oloughin, F.J. Simeone, R. Weissleder, L. Josephson, J. Am. Chem. Soc. 124 (2002) 2856.
[10] C. Xu, K. Su, H. Gu, X. Zhong, Z. Gao, R. Zheng, X. Zhang, B. Xu, J. Am. Chem. Soc. 126 (2004) 3392.
[11] S. Dai, M.C. Burleigh, Y. Shin, C.C. Morrow, C.E. Barnes, Z. Xue, Angew. Chem. Int. Ed. 38 (1999) 1235.
[12] D. Zhao, J. Feng, Q. Huo, N. Melosh, G.H. Fredrickson, B.F. Chemelka, G.D. Stucky, Science 279 (1998) 548.
[13] K. Kang, J. Choi, J.H. Nam, S.C. Lee, K.J. Kim, S.W. Lee, J.H. Chang, J. Phys. Chem. B 113 (2009) 536.
[14] J. Liu, Y. Shin, Z. Nie, J.H. Chang, L.Q. Wang, G.E. Fryxell, W.D. Samuel, G.E. Exarhos, J. Phys. Chem. A 104 (2000) 8328.
[15] J.H. Chang, K.J. Kim, Y.K. Shin, J. Liu, Chem. Lett. 33 (2004) 1204.